

Summary on machine to model comparison

This report reviews the comparison between machine and model presented at the “Nonlinear Beam Dynamics Workshop”. It is based on the comparison of the physical quantities for which both experimental and model data were available.

1. Comparison of Storage Ring Optics

Linear Optics

It was generally agreed that the linear optics of the synchrotron light sources represented at the workshop is in very good agreement with the model. It was acknowledged that LOCO or similar fitting algorithm have enormously eased the achievement of the nominal linear lattice parameter.

The β -beating reported at various light sources is 1% or less. The recent development of the LOCO algorithm to include additional constraints on the variability of the quadrupole gradients during the fit has significantly reduced the spread in the quadrupole gradients necessary to achieve the above. The above β -beating is achieved with a quadrupole variation of the order of 1%, compatible with random errors in gradients of the quadrupole.

Nonlinear Optics

The comparison of the nonlinear optics is still far from the accuracy achieved for the linear optics.

Firstly, a discrepancy in the behaviour of the various codes

- AT
- BETA-ESRF
- BETA-SOLEIL
- Elegant
- MAD-PTC
- MAD-X
- TRACY-II SLS
- TRACY-II SOLEIL
- TRACY-III

was highlighted. It was pointed out that different answers are likely to be the consequences of different assumptions used in the codes and that should be adequately considered. Nevertheless a “black box” approach was agreed as a first test, to verify the level of agreement of the codes. The Diamond lattice was proposed as a bench test given its similarity with the TPS and SSRF lattices.

It was recognised that a careful modelling is mandatory: factors like edge focussing, fringe in magnetic elements (dipoles but also quads etc.), systematic multipolar errors in main magnets (e.g. sextupole in dipole, octupoles in quads etc) cannot be neglected. The consensus on the modelisation of the ID with the kick maps formalism was widespread.

Secondly, it was suggested that a “road-map” should be followed to qualify the comparison machine to nonlinear model, indicating the physical quantities characterising the nonlinear optics. The physical quantities discussed during the workshop were

- Nonlinear dispersion
- Detuning with momentum
- Detuning with amplitude
- Apertures (on and off momentum)
- Lifetime
- Frequency Maps ($x-z$ and $x-dp/p$)
- Resonance driving terms
- Chromatic phase advance

Each facility presented the results of the measurements performed to characterise the nonlinear beam dynamics.

2. Review of linear optics comparison

SOLEIL achieved a residual β -beating 0.3% rms. The variation of quadrupole gradient is less than 1% consistent with magnetic measurements of quadrupole gradients and DCCT calibration of individual power supplies;

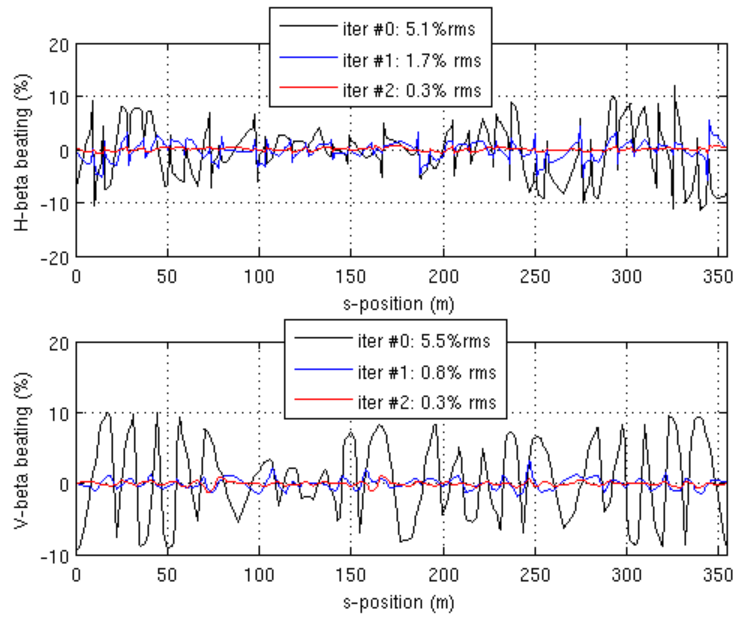


Fig. 1.1: SOLEIL residual β -beating after LOCO correction

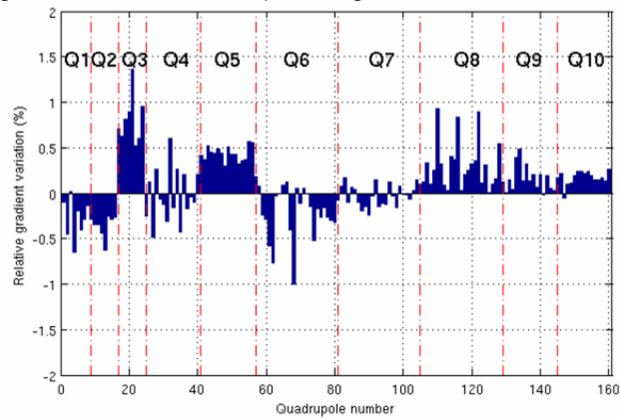


Fig. 1.2: SOLEIL relative variation of quadrupole gradients after LOCO correction

SSRF is still under commissioning however it has already achieved a β -beating less than 2% peak-to-peak. The variation of quadrupole gradient is less than 1%.

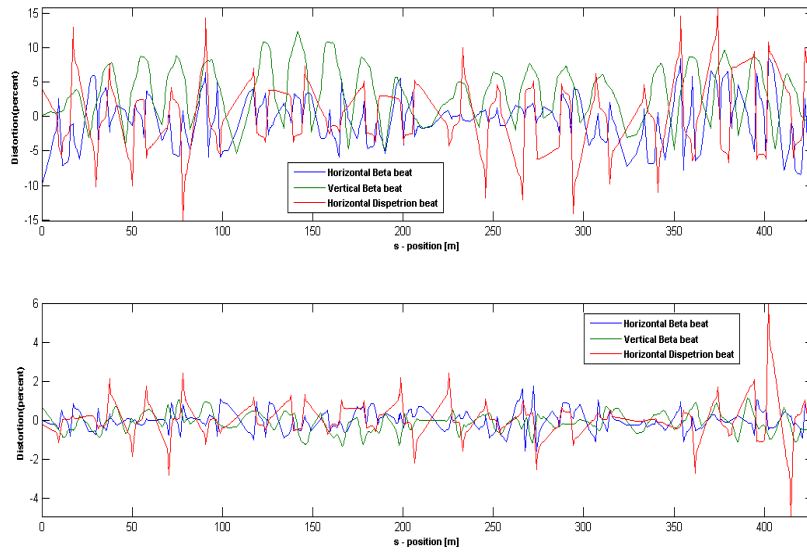


Fig. 1.3: SSRF residual β -beating after LOCO correction per family (top) per individual quadrupole (bottom)

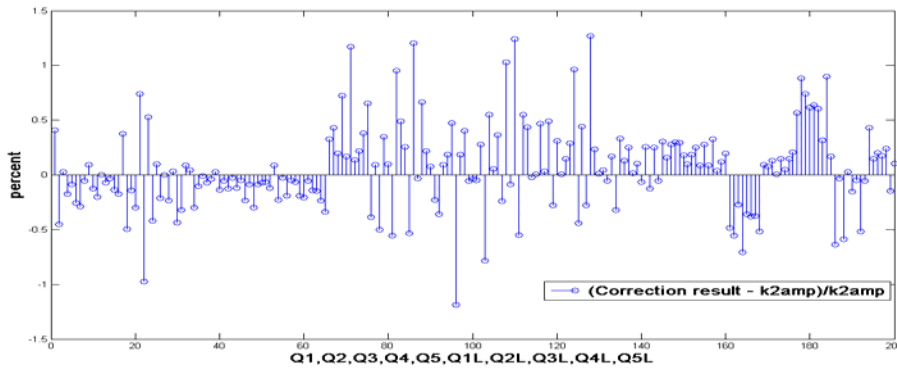


Fig. 1.4: SSRF relative variation of quadrupole gradients after LOCO correction

ESRF has corrected the optic with an approach similar to LOCO where the linear optic is reconstructed from the orbit response matrix. The result achieved is few % residual β -beating peak-to-peak in both planes with a very small variation of the quadrupoles gradient (less than 0.3%).

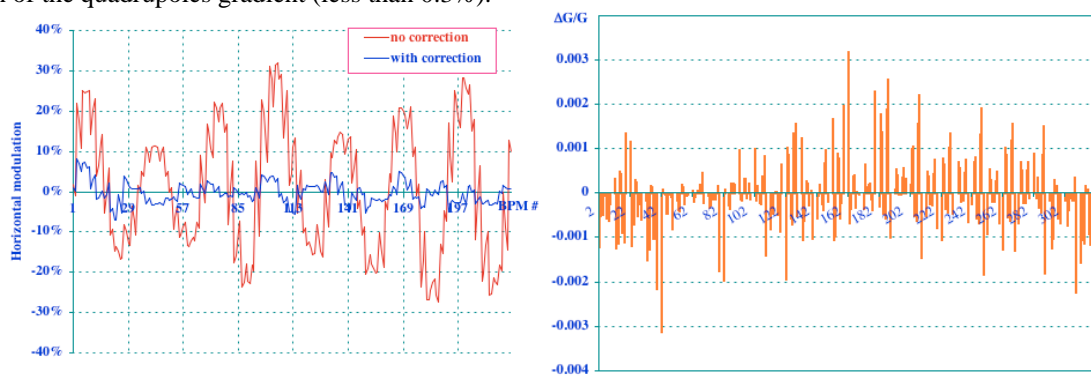


Fig. 1.5: ESRF β -beating correction (left) and corresponding variation of the quadrupoles gradient (right)

Diamond achieved a residual β -beating less than 1% peak-to-peak. The variation of quadrupole gradient is less than 1% consistent with magnetic measurements of quadrupole gradients; without constraints the LOCO predicted variation of the quadrupole peaked to 4%;

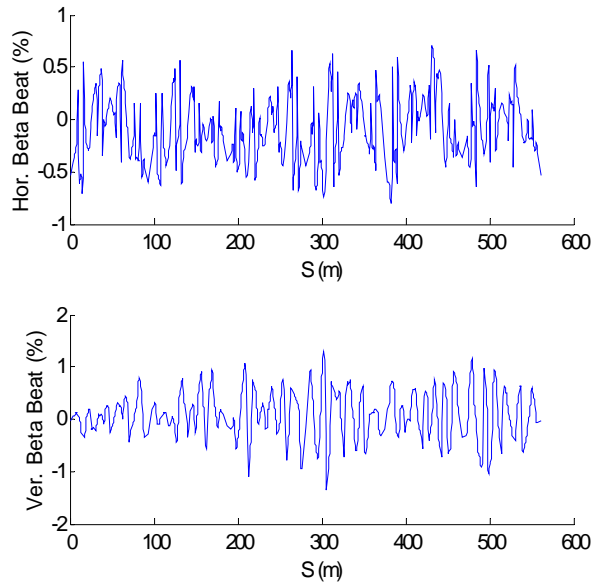


Fig. 1.6: Diamond residual β -beating after LOCO correction horizontal (top) vertical (bottom)

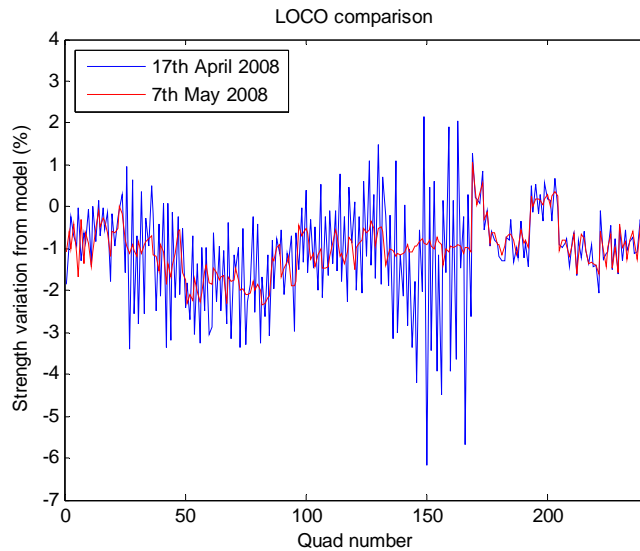


Fig. 1.7: Diamond relative variation of quadrupole gradients after LOCO correction; version without constraints (17 Apr 2008) Version with constraints (7 May 2008)

3. Review of Nonlinear Optics comparison

Review of natural chromaticity

SOLEIL: model -53, -23 measured -51.5, -19.4

Differences in the vertical natural chromaticity are due to the incorrect treatment of the off-momentum dependence of the dipole fringe fields. The natural chromaticity measurement required an NMR probe to measure correctly the dipole magnetic field variation. Early measurements based solely on the calibration curve of the dipoles generated wrong results also on the horizontal natural chromaticity.

Diamond: model -79, -35; measured -68, -28

Diamond measurements of the natural chromaticity suffer very likely from the same problems highlighted as SOLEIL.

Review of detuning with momentum (high order chromaticity)

Detuning with momentum measured at the ESRF shows a good qualitative agreement with the measurements although the difference in the vertical at $dp/p = 3.5\%$ is larger than 0.5. Edge focussing, fringe in dipoles and quadrupoles were considered in the simulations.

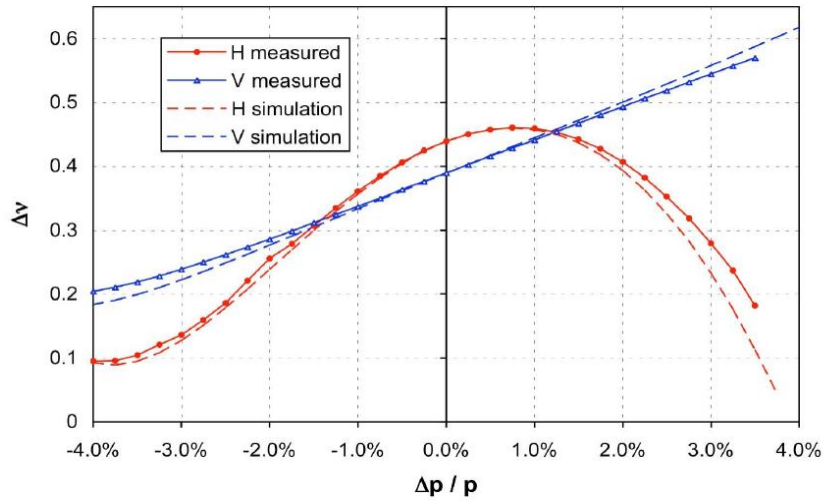


Fig. 2.1: detuning with momentum at ESRF for the nominal working point

SPring-8 performed thorough comparisons between measurements, analytical formulae and simulations reporting a good agreement among these.

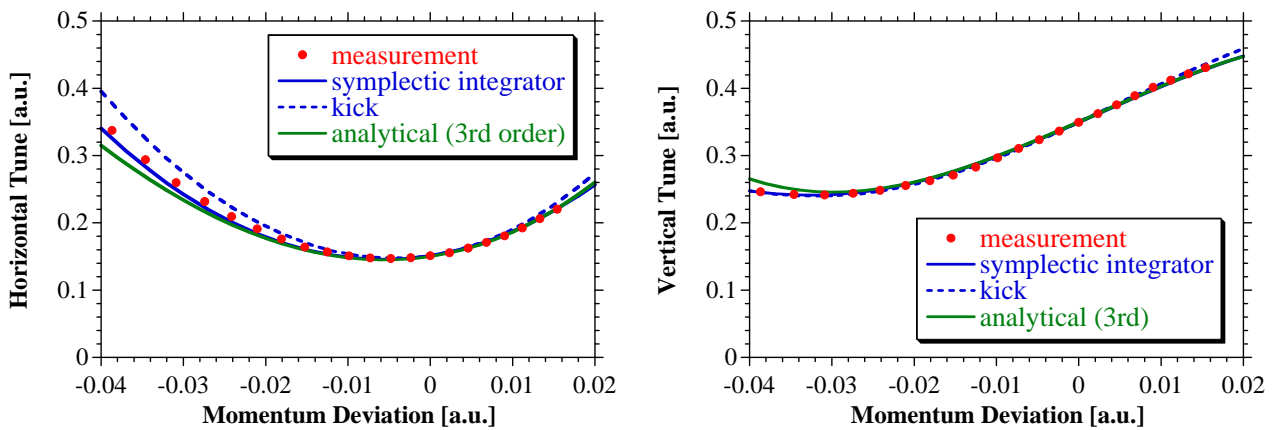


Fig. 2.2: Spring-8 nonlinear detuning with momentum

Diamond studies on nonlinear chromaticity show that a satisfactory agreement can be achieved if the calibration factors of the sextupoles magnet are used as fit parameter for the match. So far it was not possible to match simultaneously the detuning with amplitude and the detuning with momentum with the sextupole calibration factor.

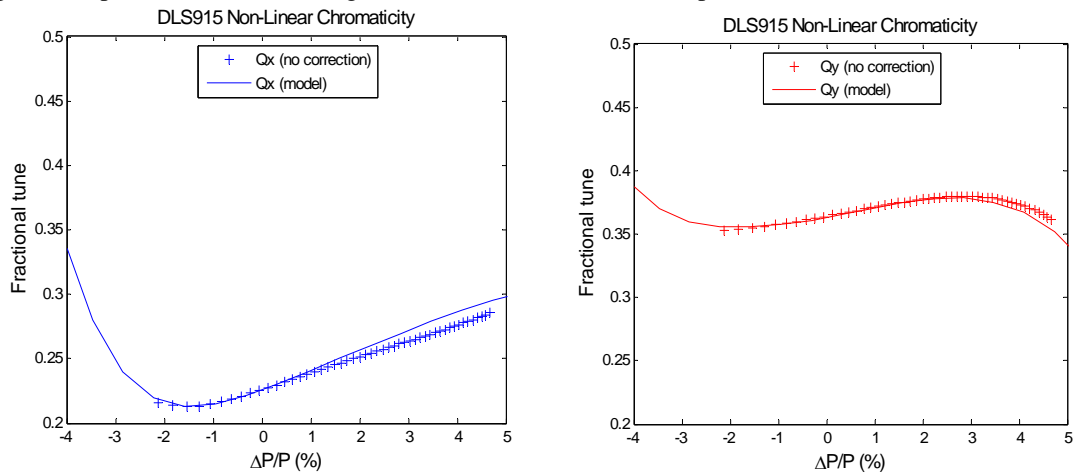


Fig. 2.3: Diamond detuning with momentum: horizontal (left) and vertical (right)

SOLEIL reported a very good agreement on a lattice with chromaticities +3 in both planes up to a dp/p of $\pm 3.5\%$. The measured values are limited at positive off momentum by an integer resonance and at negative off-momentum by loss on the longitudinal dynamics.

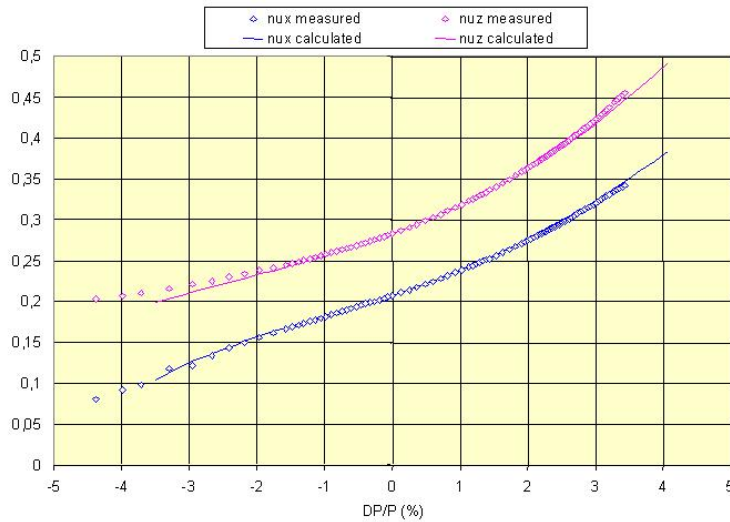


Fig. 2.4: SOLEIL detuning with momentum for a lattice with chromaticity +3 in both planes.

SPEAR3 has measured the detuning with amplitude with pinger experiments. Once the values of the chromaticity of the model are set to the measured values by means of a calibration factor in the sextupoles then detuning with momentum curves agree quite well in the horizontal plane less so in the vertical.

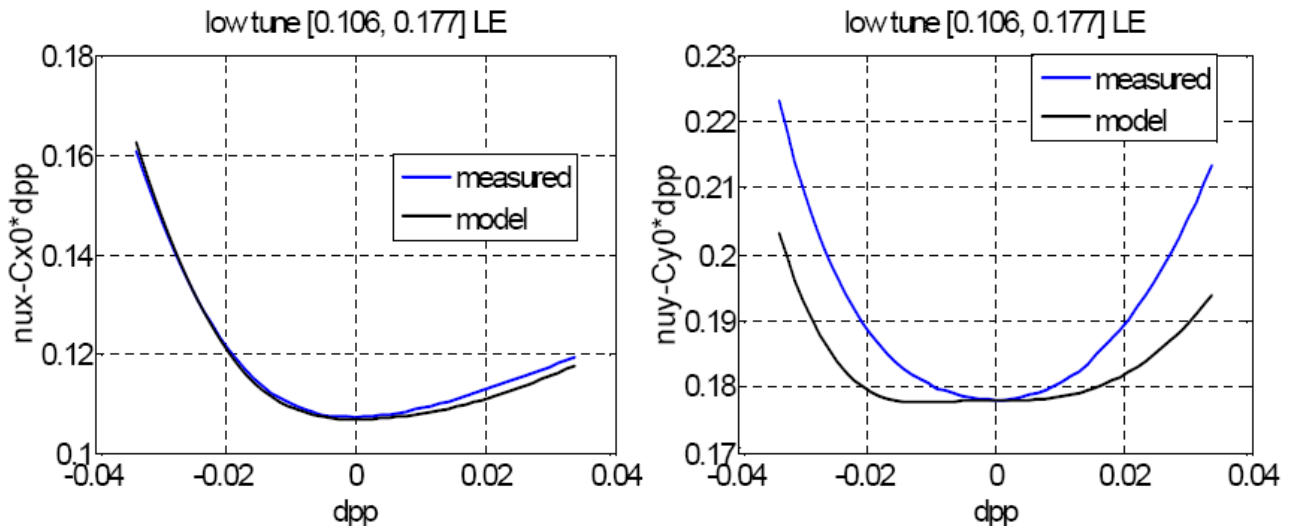


Fig. 2.5: SPEAR3 higher order chromaticity terms for the low-emittance low tune lattice. Horizontal (right) vertical (left)

Review of momentum apertures

Momentum apertures are measured with scans of lifetime vs RF cavity voltage or with Tosuchek lifetime measurements. Momentum apertures are generally smaller than predicted by the numerical simulations. Tab. 1 summarises the results reported at the workshop. One can conclude that the agreement is reasonable although not excellent. The SLS appears to be the farthest from the predicted momentum aperture..

Machine	Measured aperture	Model Aperture
BESSY-II	2.5%	$\pm 3\%$ (RF)
Diamond	3.5%	- 5% to 3.5% (RF + α_2)
ESRF	2.4%	$\pm 2.5\%$ (RF)
SLS	1.8%	$\pm 3\%$ (RF)
SOLEIL	- 4.6% to 3.5%	- 6% to 3.8% (RF + α_2)
SPEAR3	$\pm 3\%$ (RF)	$\pm 3\%$ (RF)

Tab. 1: Summary of momentum apertures measurements

At Diamond the simulations including coupling errors to 0.2% and multipole errors in the quadrupoles predict a momentum aperture of 3.5 % (at 2.6 MV). The momentum aperture measured with lifetime scans vs RF voltage is in good agreement.

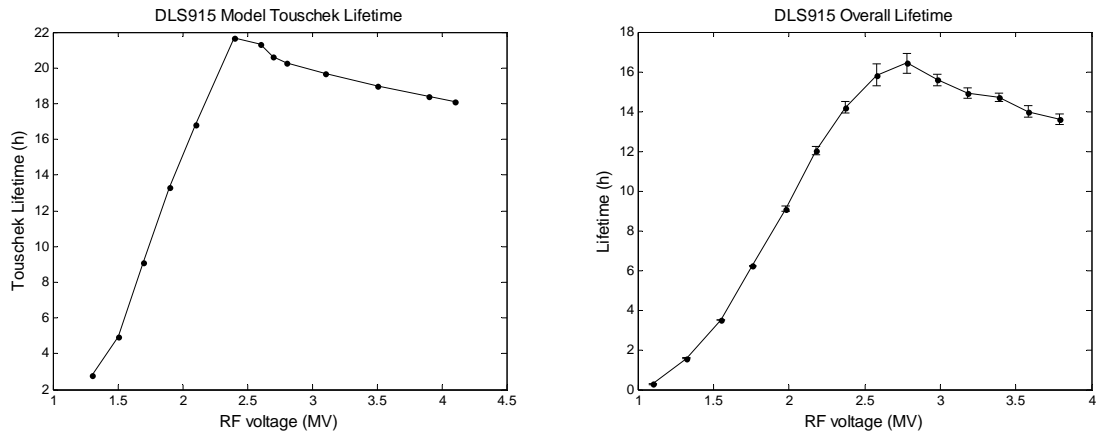


Fig. 2.6: Momentum aperture with lifetime vs RF voltage scan: simulated (left) measured (right)

The lifetime vs RF voltage scan at ESRF show a momentum aperture of 2.4% which is close to the nominal 2.5%, however the lifetime values required the adjustment of the bunch length by a factor 0.75 to match the simulations. The lifetime refer to single bunch with low coupling.

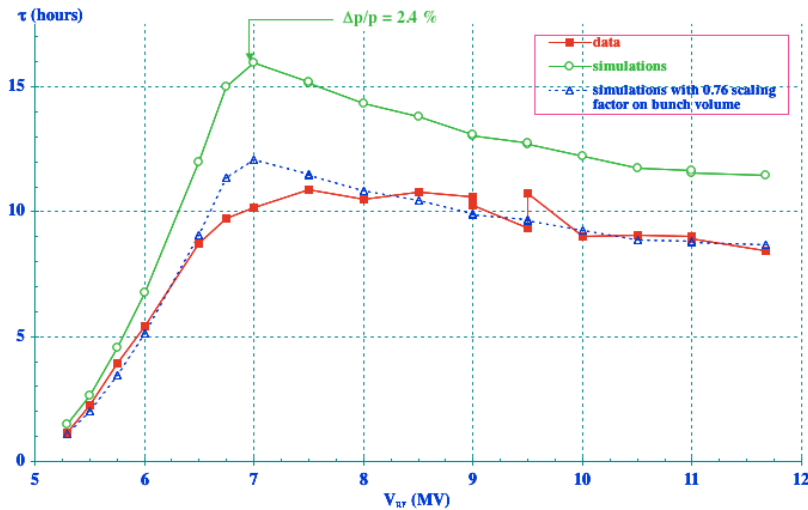


Fig. 2.7: ESRF momentum aperture with a scan lifetime vs RF voltage

At BESSY-II the lifetime vs RF voltage scan show a momentum aperture of 2.5%. The effect of the four SCW is not particularly visible.

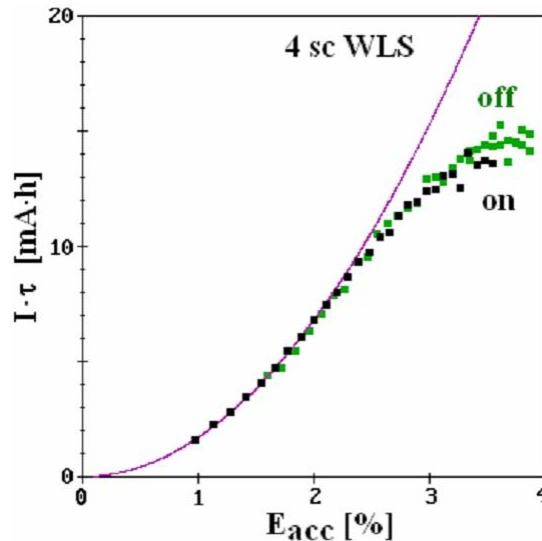


Fig. 2.8: Bessy-II momentum aperture with a scan lifetime vs RF voltage

At SOLEIL the momentum aperture was inferred from the lifetime measurements and is predicted to be -4.6% to 3.5% due to the strong effect of the second order momentum compaction α_2 . The agreement with the theoretical -6% to 3.8% is satisfactory.

At SPEAR3 the momentum aperture was investigated both with lifetime vs RF voltage scan and with lifetime measurements. It is in excellent agreement with the expected RF aperture of 3% .

Review of transverse apertures

Transverse aperture are measured with scrapers or by probing the maximum available aperutre with kick excitations. The equivalence of the two methods is not fully clarified. Tab. 2 summarises the results reported at the workshop.

Machine	H aperture	V Aperture
BESSY-II	10 mm (septum at 12.1 mm)	limited by ID gap to 2.1 mm
Diamond	11.4 mm limited by DA	2.7 mm (5 mm with scraper)
ESRF	<15 mm instead of 16.5 mm; limited by DA	3.1 mm instead of ± 4 mm; limited by DA
SLS	Ax 11 mm mrad instead of 30 mm mrad	limited by ID gap 1.8 mm
SOLEIL	18.6 mm limited by absorber	4.8 mm instead of 5.5 mm; limited by ID 5 mm gap
SPEAR3	12.9 mm instead of 15 mm	4 mm instead of 6 mm

Tab. 2: Summary of transverse apertures measurements

At the ESRF the horizontal aperture has been probed measuring the lifetime as a function of the position of a collimator. The physical apertures are defined by the septum at 19 mm and the narrow ID gap at ± 4 mm. Measurements performed on several different optics have shown that the horizontal aperture at the scraper is always below 15 mm and is smaller than the corresponding scaled aperture at the septum (16.5 mm at the scraper). Therefore the septum is not the limiting factor. The reason for this discrepancy is not fully understood.

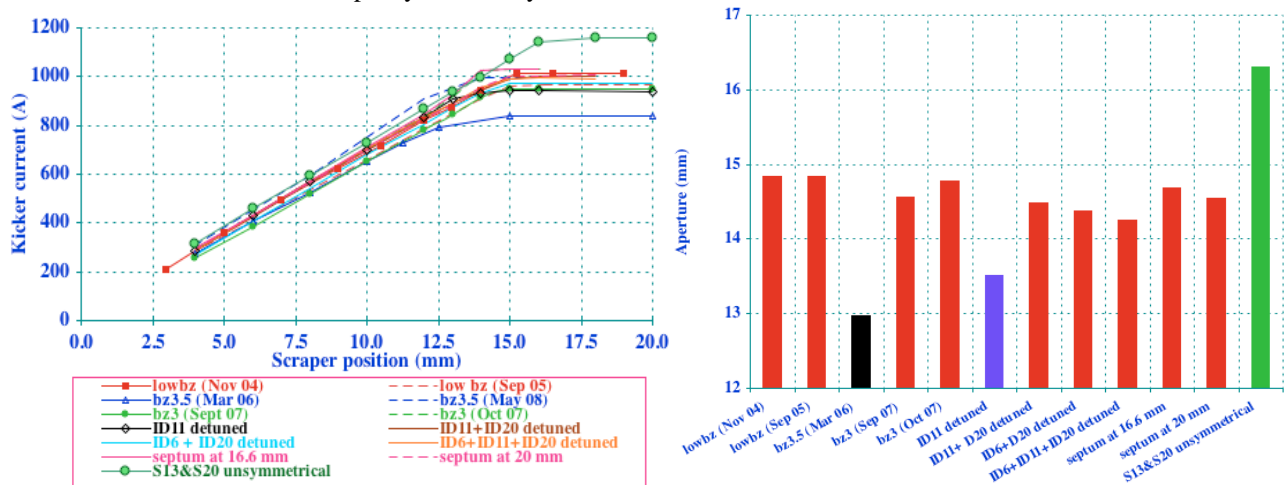


Fig. 2.9: ESRF horizontal aperture. Scraper. Horizontal aperture comparison (right)

In the vertical plane the aperture was measured using a scraper and measuring the reduction of the lifetime. The aperture at the scraper is 8 mm vertically. Scaled at the ID, this corresponds to about 3.1 mm which is significantly less than the 4 mm expected from the narrow gap vessel.

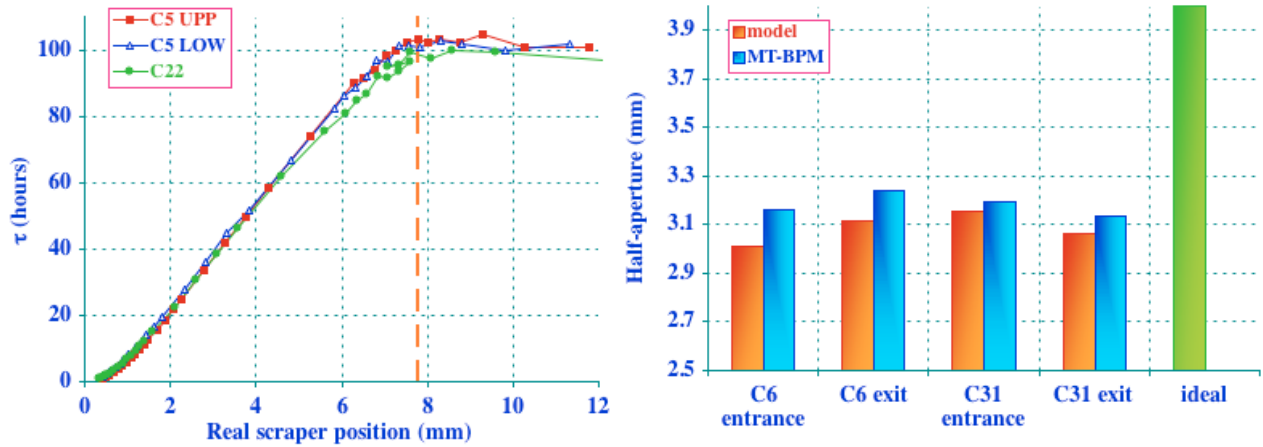


Fig. 2.10: Vertical aperture scan at the ESRF (left) and aperture corresponding aperture at the narrow gap ID location (right)

At Diamond the aperture were measured both with a scraper and with kicking the beam to large amplitude with the pinger magnets. Both apertures are lower than predicted by the model and this discrepancy is under investigation and is likely to be due to a dynamic aperture problem. Scraper and pinger data agree in the horizontal plane (about 11 mm) while the kicked beam give a significantly lower vertical aperture (2.7 mm) than the scraper (about 5 mm). N.B the scraper data were not shown at the workshop.

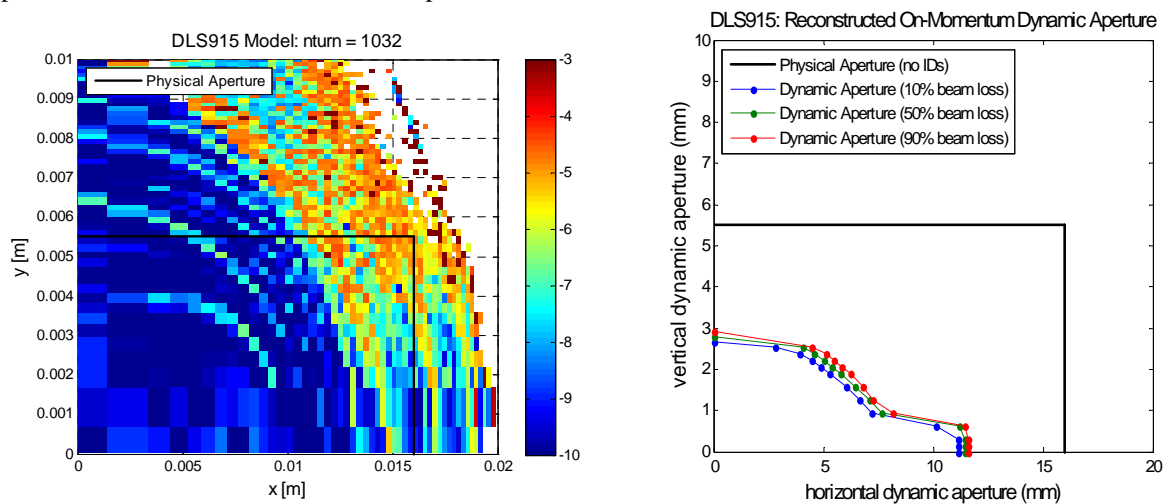


Fig. 2.11: Diamond DA (left) and measured on momentum aperture in both planes (right)

At SOLEIL the vertical aperture was measured with a scraper located in a long straight section and recording the product lifetime times the average current as a function of the scraper position. The measured vertical aperture is 4.8 mm while 5.5 mm are expected from the projection of the ± 5 mm limiting vertical aperture of the ring.

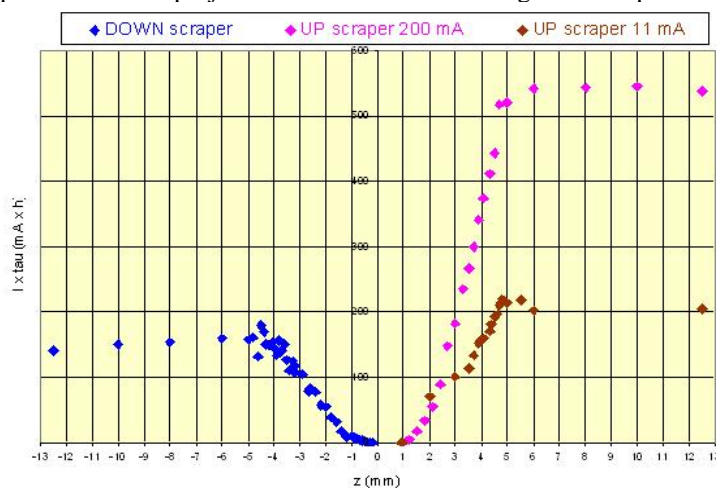


Fig. 2.12: SOLEIL vertical aperture measured with a scraper.

The dynamic aperture at SOLEIL was also measured with pinger magnet excitation. The results on the lattice with zero chromaticity show that the vertical aperture is slightly smaller than predicted while the horizontal limit at 18.6 mm are consistent with the position of an absorber upstream the U20.

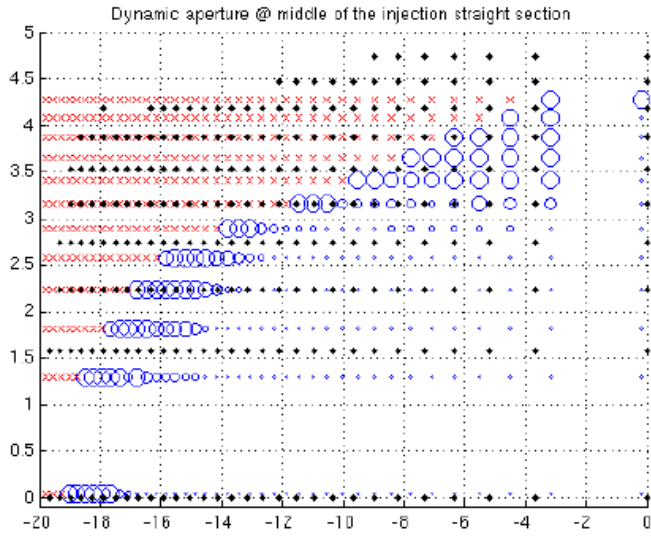


Fig. 2.13: SOLEIL measurement of DA with zero chromaticities.

At BESSY-II the vertical and horizontal aperture were measured both with scrapers and with pinger excitation. A vertical aperture of 2.1 mm is expected from the small vertical gap ID chamber. In the horizontal plane the aperture is limited to about 10 mm limited by the femtoslicing set up not by the septum at 12.1 mm.

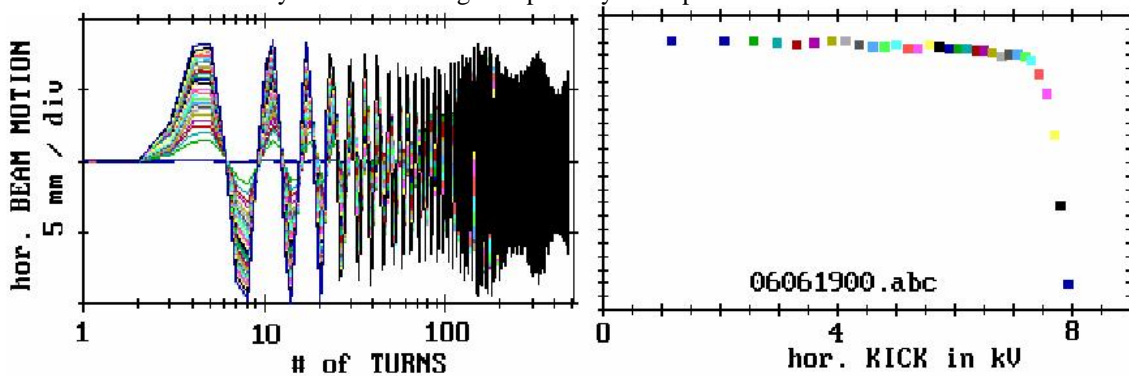


Fig. 2.14: Horizontal aperture at BESSY-II measured with pinger magnet excitation

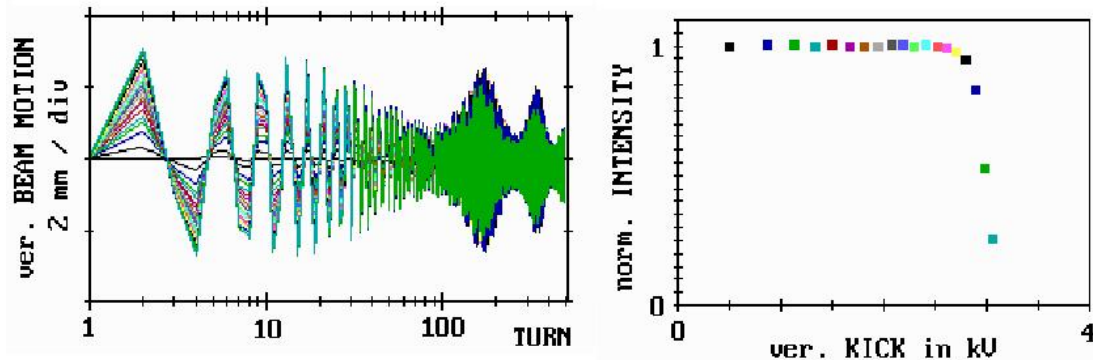


Fig. 2.15: Vertical aperture at BESSY-II measured with pinger magnet excitation

At SLS the vertical aperture is measured by means of scrapers. The horizontal acceptance is measure to be between 1.6 and 1.8 mm mrad which is consistent with the 2 mm mrad expected from the narrow gap vessel in the modulator of the femto-slicing set up. The lifetime is not limited by the vertical gap and there is a request to go down to 4 mm gap with the in-vacuum undulators.

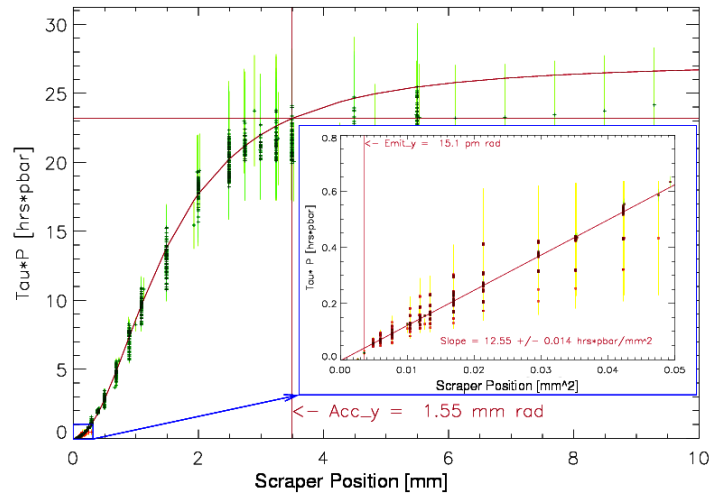


Fig. 2.16: SLS vertical aperture measured with scrapers

The horizontal acceptance is measured with a pinger magnet and it is 11 mm mrad significantly less than the 30 mm mrad predicted by the simulations for the ideal lattice. SLS has investigated also the vertical aperture with scraper at small coupling (0.4%): while again the vertical aperture is not the limit for the Touschek lifetime, in the horizontal the effect of the chromaticity on the aperture is significant. A good agreement with the modelled is recovered for the low chromaticity low coupling case.

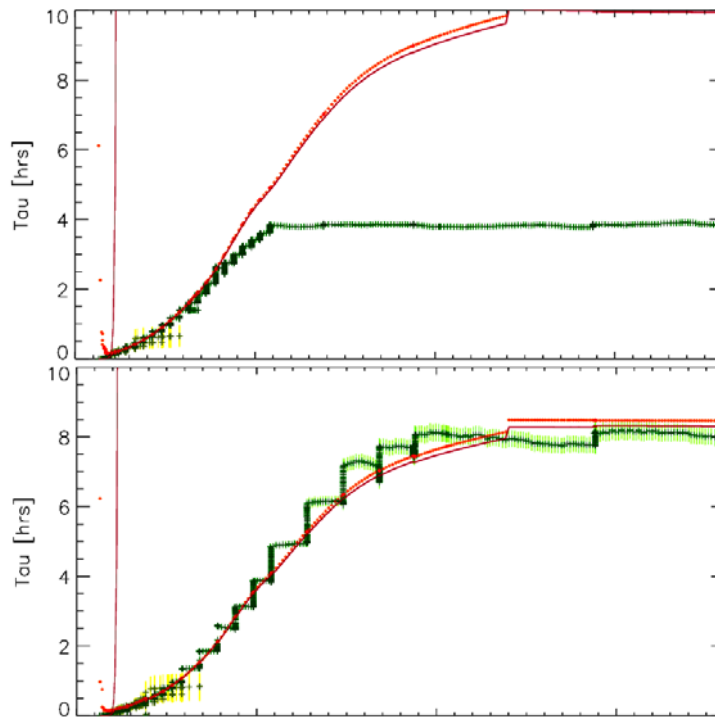


Fig.2.17: SLS horizontal aperture measured with a scraper: chromaticity 3.8 upper, chromaticity 0.4 lower; green measurements red Tracy-II simulations

SPEAR3 has measured the horizontal dynamic aperture with horizontal kick scans for on and off-momentum. The measured value is 8 mm at a BPM with $\beta_x = 3.46$ m. The septum is at $\beta_x = 9.02$ m therefore the DA at the septum is 12.9 mm which is smaller than the 14-15 mm predicted by the simulations.

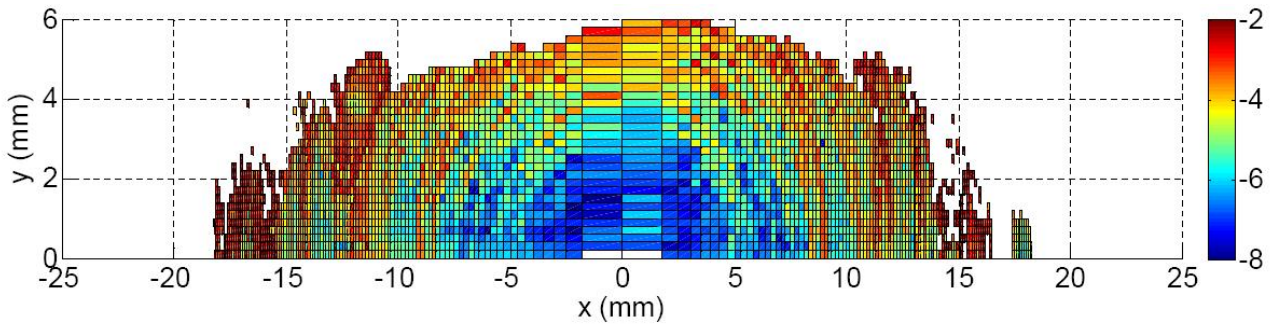


Fig. 2.18: SPEAR3 predicted DA for the low emittance low tune lattice. Horizontally it extends to 15mm $\beta_x = 9.02m$

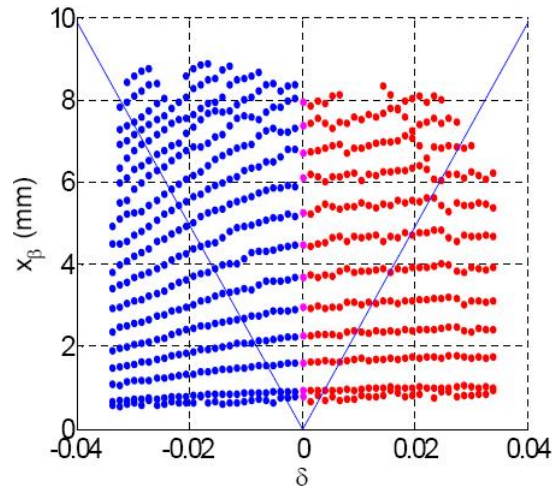


Fig. 2.19: SPEAR3 measured horizontal DA with off frequency kicks. The magenta dots refer to on-momentum energy and it extends to 8 mm for a $\beta_x = 3.46m$.

Review of transverse off-momentum apertures

At ESRF the transverse aperture was measured by changing the RF frequency and measuring the loss rate to define the aperture. The measurements show a dip at -1% not understood and existing for all lattices tuned at $Q_x = 0.44$ $Q_y = 0.39$; possible candidates are the resonance $Q_x + 2Q_y$ or the node $Q_x = Q_y = 0.33$; Extra tuning with a sextupole helped removing the dip (still under investigation).

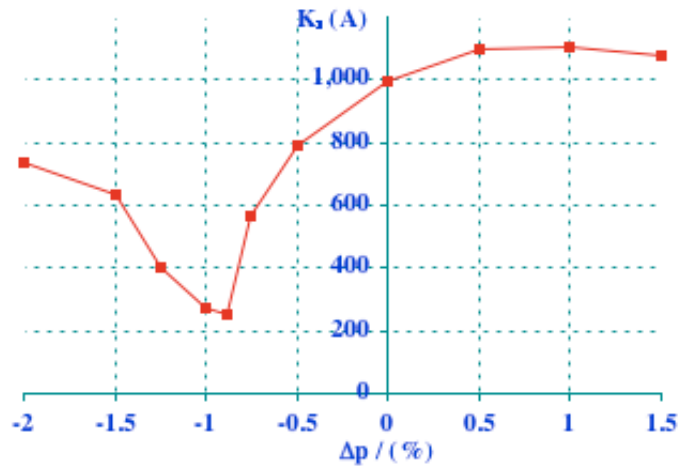


Fig. 2.20: ESRF transverse aperture as a function of the off-momentum

SPEAR3 has measured the horizontal dynamic aperture with horizontal kick scans for on and off-momentum. Data on the comparison with the off-momentum DA are available only at $dp/p = 2\%$ where the agreement is good taken into account the β functions.

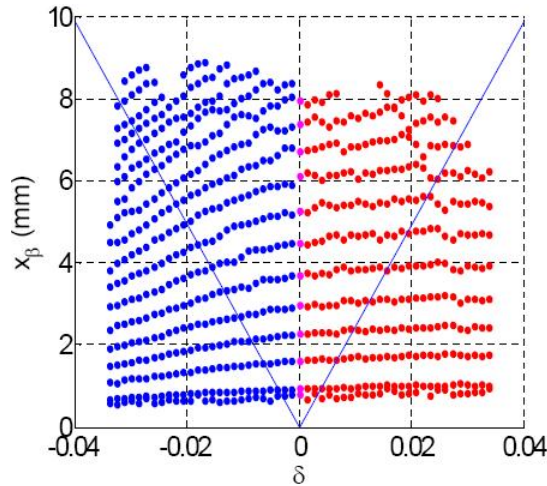


Fig. 2.21: Same as Fig. 2.17, the accent now is on the off-momentum information

Review of Touschek lifetime

Lifetime is limited by apertures (dynamic or physical depending on the machine)

Machine	Measured lifetime	Model lifetime
BESSY-II (240 mA)	10 h (all)	-
Diamond	16 h (all)	22 h
ESRF (single bunch, low coupling, $dp/p = 2.4\%$)	11 h (all)	16 h
SLS ($dp/p = 1.8\%$, $chro = 0.4$, $coup = 0.4\%$)	8 h (Touschek)	8 h
SOLEIL (250 mA, 312 bunches, $k = 0.9\%$, 2.4 MV; $dp/p = -4.6\%$; 3.5%)	17.3 h (Touschek)	16.4 h
SPEAR3 (100 mA, 280 bunches, $k = 0.1\%$, 3.2 MV, $dp/p = \pm 3\%$)	61.3 h (Touschek)	66.3 h

At diamond the lifetime was measured as a function of the RF voltage. It peaks at 16 h for 2.6 MV. Taking into account the elastic gas lifetime contribution 120 h it agrees well with the simulations which off 22 h Touschek lifetime.

The ESRF lifetime measured in single bunch at low coupling is 11 h. The simulations require a reduction of the bunch volume of 0.75 to match the measured value.

SLS lifetime depends strongly on the chromaticity and can be summarised at

$$T \approx 14 \text{ hrs } (k[\%])^{1/2} / I_b[\text{mA}] \quad \text{at chromaticity } 1$$

$$T \approx 6 \text{ hrs } (k[\%])^{1/2} / I_b[\text{mA}] \quad \text{at chromaticity } 5$$

The agreement with the simulation is good for the case with low chromaticity 0.4 and low coupling while it is worse for the other configuration.

At SOLEIL there is a very good agreement between the simulated lifetime and the measured one 17.3 h measured and 16.4 h predicted by the model.

SPEAR3 reported the measurement and simulation of the Touschek lifetime by means of the 6D tracking computation of the momentum aperture. The agreement is very good for two different types of lattices, the double waist (DW) and low-emittance (LE). The measured values for the Touschek lifetime were 91.3 h (96.7 h predicted) for the DW lattice and 66.3h (61.3 h predicted) for the LE lattice.

Review of Frequency Maps

At Bessy-II FM were extensively used to improve the performance of the SR. Comparison with the model were performed earlier on the bare model and reported elsewhere.

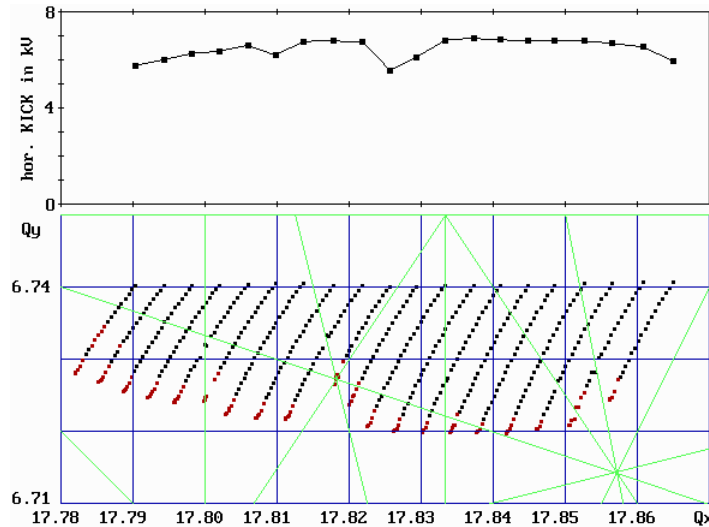


Fig. 2.22: Working point optimisation studies performed with FM at BESSY-II

Frequency maps were measured at ESRF since 2002. Horizontal oscillations are excited with the injection kickers while vertical oscillations are excited with a shaker. The small vertical aperture limits significantly the area explored by the frequency map. The detuning is in good agreement while the effect of the 5th order resonance $5Q_y = 2$ is underestimated in the model.

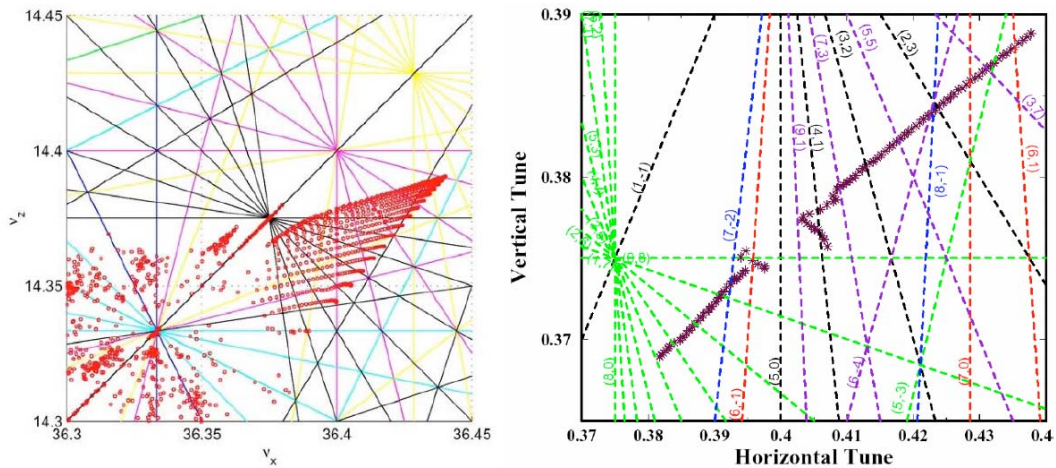


Fig. 2.23: ESRF FM. Model (left) measured (right)

More recent FMs have been measured in 2008 with correction applied on a new lattice with doublets instead of triplets. The effect of the 5th order resonance is less important.

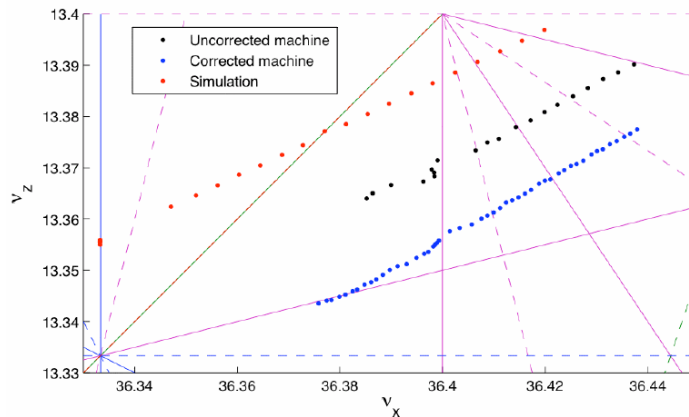


Fig. 2.24: ESRF new lattice measured FM

At Diamond FM have been measured and calibration factor for the sextupole were used to fit the FM. There is qualitative agreement.

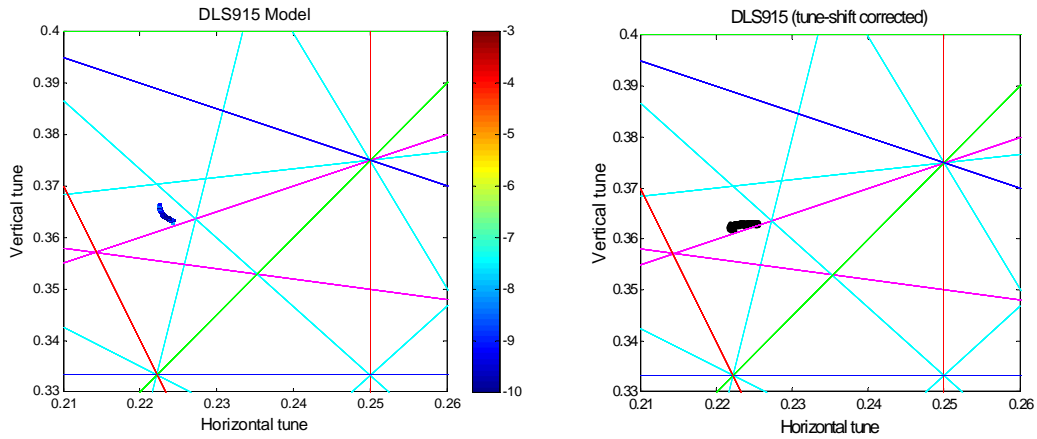


Fig. 2.25: Diamond FM. Numerical (left) measured (right)

At SOLEIL preliminary FM studies show already a qualitative agreement between machine and model.

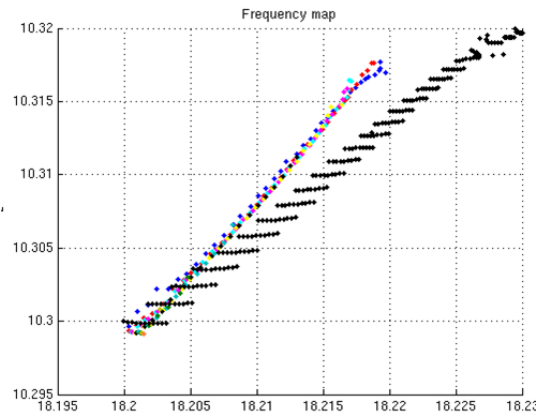


Fig. 2.26: FM at SOLEIL: black is numerical simulations, coloured dots are measured data

Review of driving term measurements

Resonant driving terms were measured at diamond: the (3,0) and (1,2) resonant driving term were targeted for correction.

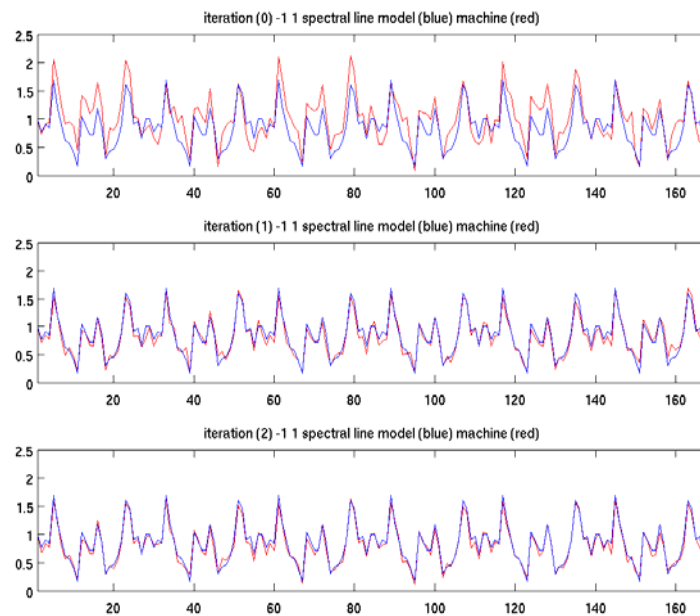


Fig. 2.27: Measurement and comparison of spectral line at Diamond

Similar experiments were performed at the CERN SPS

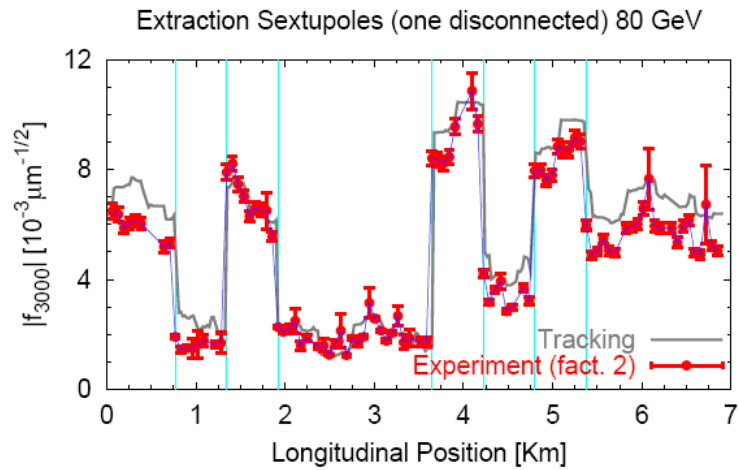


Fig. 2.28: Measurement and comparison of spectral line at CERN-SPS

Review of effect of IDs

At Bessy-II the effect of the ID was analysed with FM and a very good and it was used to improve the performance of the IDs after shimming

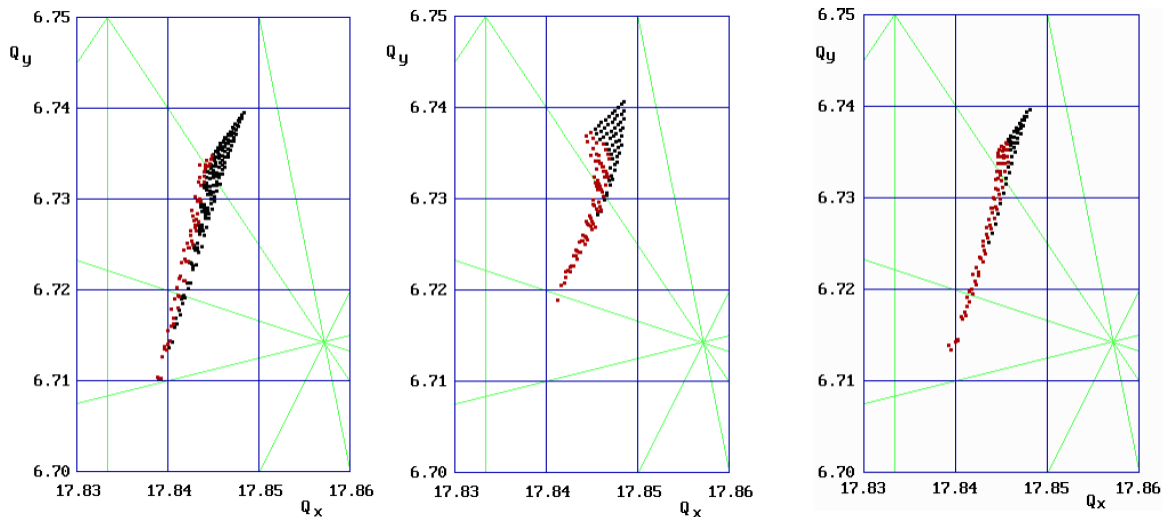


Fig. 2.29: FM comparison at BESSY-II: open ID gap (left), closed ID gap before correction (centre), closed ID gap after correction (right);

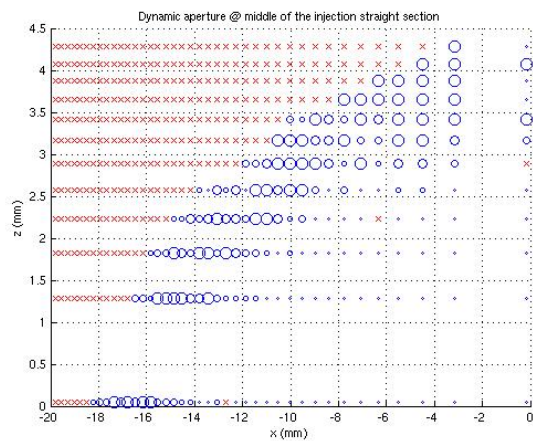


Fig. 2.30: SOLEIL bare lattice

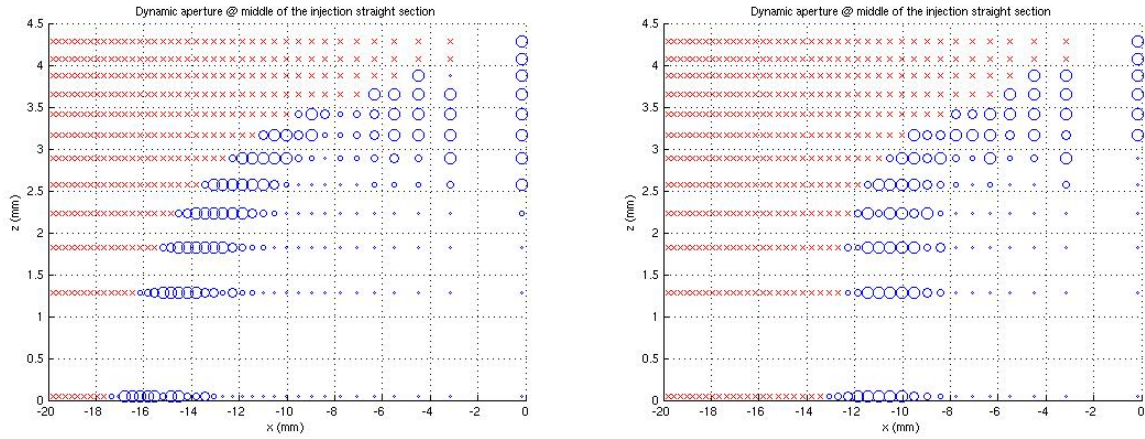


Fig. 2.31: DA with a single U20 (left) ; DA with three U20 (right)

At SOLEIL it was found that the ID have a significant effect on the injection efficiency and lifetime (60 mA, 8 bunches, coupling 6.5%) as reported in Tab. 3. The DA measurements and simulation reflect the reduction of the DA with three U20 closed simultaneously.

Bare lattice	98%	13.1 h
One U20	88 %	12.8 h
Three U20	55%	8.7 h

Tab. 3: Injection efficiency at SOLEIL with ID closed

At SPEAR3 the DA was measured by exciting betatron oscillations. It is measured to be 13 mm w.r.t. the theoretical 15 mm for the Low tune low emittance lattice. At the same time FM were measured and compared to the theoretical. The IDs were modelled with Halbach analytical formulae. The detuning with amplitude, especially the cross terms do not agree particularly well with the model.

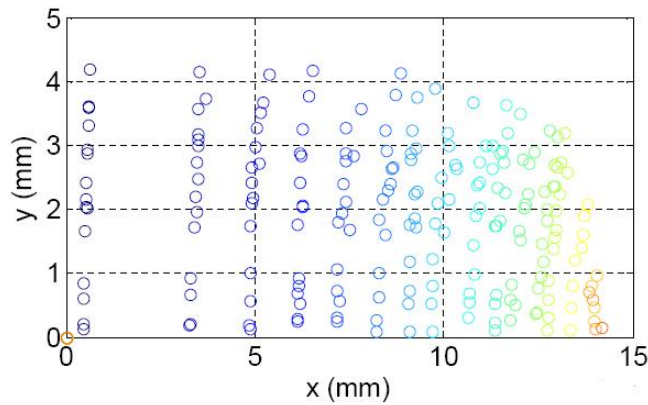


Fig. 2.32: SPEAR3 DA with ID closed

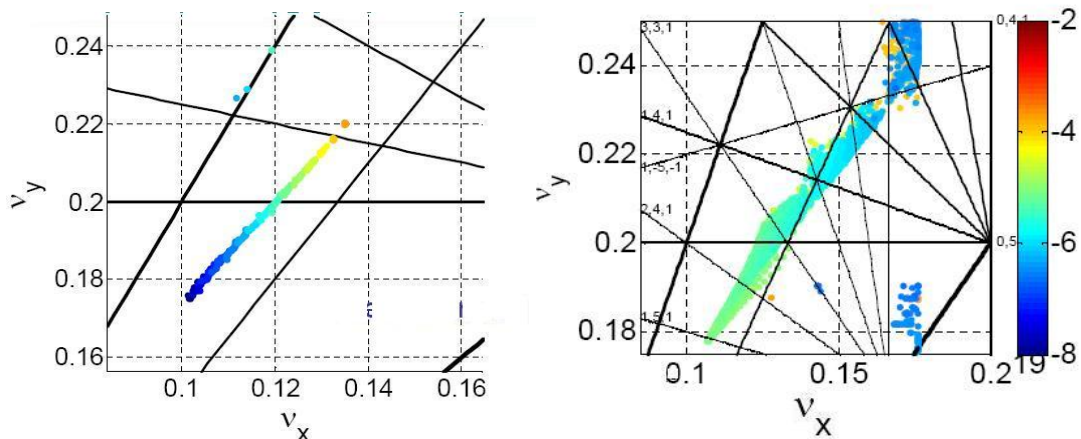


Fig. 2.33: SPEAR3 with ID closed. Comparison of FM

At SPring-8 the effect of the IDs was investigated mainly in terms of their effect on the injection efficiency with the U19 closed. The agreement with the simulation is quite good.

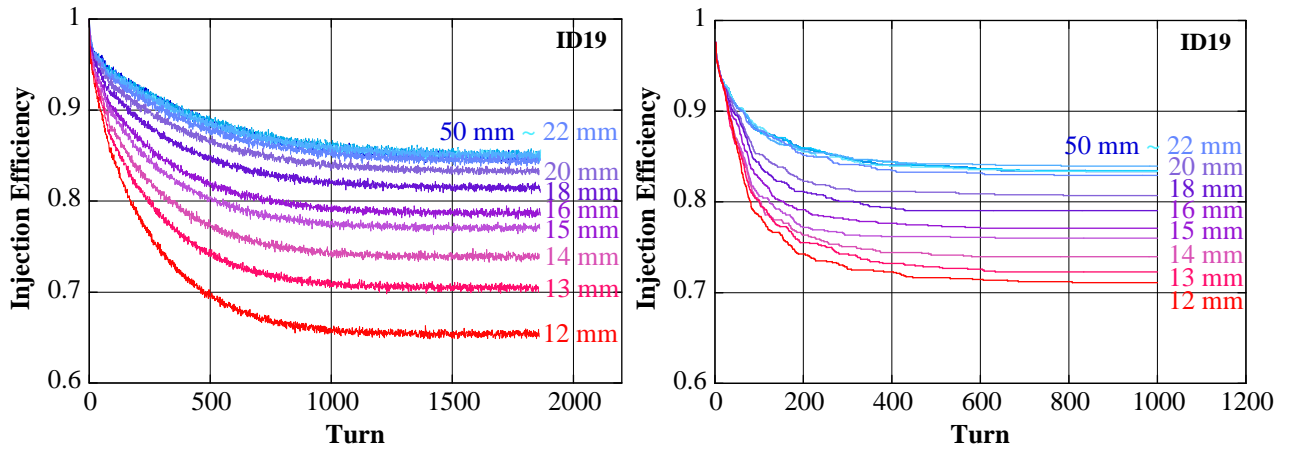


Fig. 2.34: Spring-8: Measurements and simulations